Electrolysis of Cryolite-Alumina Melts on Solid Cathodes

Evgeniy S. Gorlanov
LLC "Expert-Al", deputy general director
86 A, Sredny Prospect, 199106, St. Petersburg, Russia
Corresponding Author: gorlanov@yandex.ru

Abstract

Attempts of the electrochemical synthesis of titanium diboride (TiB2) coatings on a carbon cathode in a cryolite melt and the subsequent study of the surface by electron microscopy made it possible to establish the cause of the unsatisfactory quality of cathode precipitation and instability of the electrolysis process. The cause is the chemical and physical inhomogeneity of the surface of polycrystalline cathodes. Point depressions, closed and open porosity, microcracks, fractures and surface folds initiate the phenomenon of “pseudo-wettability” by the mechanism of capillary phenomena, for which the conditions of occurrence and features were investigated by numerical methods. These surface defects initiate the current concentration at the micro defect sites and lead to an increase in the rate of cathodic processes with the development of concentration polarization and an increase in voltage to the decomposition potentials of cryolite, sodium fluoride and aluminum. The consequences of these negative processes are the interaction of intrinsic and impurity-aggressive elements with the surface material, the progressive development of physical micro-defects and the passivation of the cathode with refractory sediments and electrolyte components. To solve these problems, it was proposed to use the technology developed in the laboratory for boronization of composite cathodes and low-temperature synthesis of titanium diboride.

Keywords: solid electrode, chemical inhomogeneity, physical micro-defectiveness, limiting diffusion current density, surface wettability, cathode passivation.

1. Introduction

The new generation cell technology with drained cathodes and vertical arrangement of electrodes involves the use of large-sized pressed or cast electrode products made of materials that are inert or less consumed in an aggressive environment. Since Belyaev and Studentsov in the 1930s [1-3] and Ransley in the 1950s [4, 5] published their reports and patents about the advantages of using oxides, carbides and borides of refractory metals for electrodes of aluminum cells, two "aluminum revolutions" were announced. The first of these that began in 2000s from Credit Suisse First Boston Corporation [6] did not occur, but in the continuation received the appearance of a new innovative company. In May 2018, the aluminum giants Alcoa Corporation and Rio Tinto Aluminum announced the creation of the Elysis joint venture in Montreal (https://elysis.com), which plans to introduce a revolutionary electrolysis technology using inert electrodes in Canada in 2024, calling it “low carbon” [7].

Taking into account the next “aluminum revolution”, which Alcoa has been developing for about 35 years and UC Rusal has been at the threshold of introducing inert anodes for about 15 years [8], reducing its implementation time and overcoming existing problems require the support of scientific and practical potential from academic institutions. Apparently, the challenge is not only in the high cost of products from titanium diboride, but also in the features of the cathode processes on solid polycrystalline cathodes for the electrolysis of cryolite-alumina melts.

2. Electrochemical Deposition on the Cathode of Boron, Titanium and Aluminum

Theoretically, there are no formal restrictions on the reduction of titanium and boron on an inert or reactive cathode:

$$B_2O_3 + 3/2C = 2B + 3/2\ CO_2 \qquad E^0_{B3+/B} = -0.626\ V \qquad (1)$$

$$TiO_2 + C = Ti + CO_2 \qquad E^0_{Ti4+/Ti} = -0.807\ V \qquad (2)$$

The sequential reduction of titanium and boron suggests their subsequent interaction with the formation of an aluminum-wettable layer of titanium diboride:

$$Ti + 2B = TiB_2 \qquad \Delta G^0_{1300} = -320\ kJ/mol \qquad (3)$$

After the formation of a TiB_2 layer on the carbon surface, one can proceed to the electrolysis of cryolite-alumina melts according to standard technology, with a drained cathode or vertical electrodes. Attempts to implement this technology [8] in the laboratory ended with visual wetting of the carbon cathode by a layer of electrolytically deposited aluminum. However, upon a closer examination (X-ray and SEM-EDS analyses), the observed wettability is qualified as “pseudo-wettability” since the contact of aluminum with the cathode surface was occurred through an electrolyte layer of discrete thickness. It was suggested that the cause of the effect of "pseudo-wetting" is the heterogeneous surface of polycrystalline materials with numerous micro and macro irregularities, cracks and pores. For a better understanding and the solution of the problem, an investigation based on experimental work and numerical methods was carried out, and the following was determined:

- Features of electrochemical deposition and synthesis of wettable coatings and aluminum on the carbon cathode;
- Numerical study of wetting conditions for polycrystalline cathode products;
- Restrictions on the use of solid cathodes for electrolytic aluminum production;
- Perspective directions for creating aluminum-wettable coatings for the cathode design of cells.

3. Experimental Work and Discussion of Results

Electrochemical deposition of titanium, boron and aluminum was carried out for 24 hours at a calculated geometric current density of 0.82 A/cm^2 and a temperature of ~ 970 °C. A graphite crucible was used as an anode; and carbon cathodes that were milled to a diameter of 30 mm and a height of 50 mm were divided into two groups:

- Samples after milling with visually observed surface microdefects from the tool in the form of furrows, open porosity, scoring, and surges, and
- Samples with a visually smooth surface which is further carefully polished and washed in distilled water.

In the melt, on the basis of technical cryolite, borax, titanium oxide and in the final stage for 2 hours – aluminum oxide, were added. Under galvanostatic conditions, the voltage dynamics during the experiment was recorded continuously. The presence or absence of aluminum on the cathode at the end of the experiment was a visual indicator of the degree of wettability of the surface

Figure 1 shows the voltage dynamics of two of the numerous attempts to synthesize titanium diboride at the carbon cathode, followed by electrolysis of cryolite – alumina melts. In both cases, with a rough milled and polished cathode surface, the electrolysis processes are unstable with a significant voltage fluctuation.

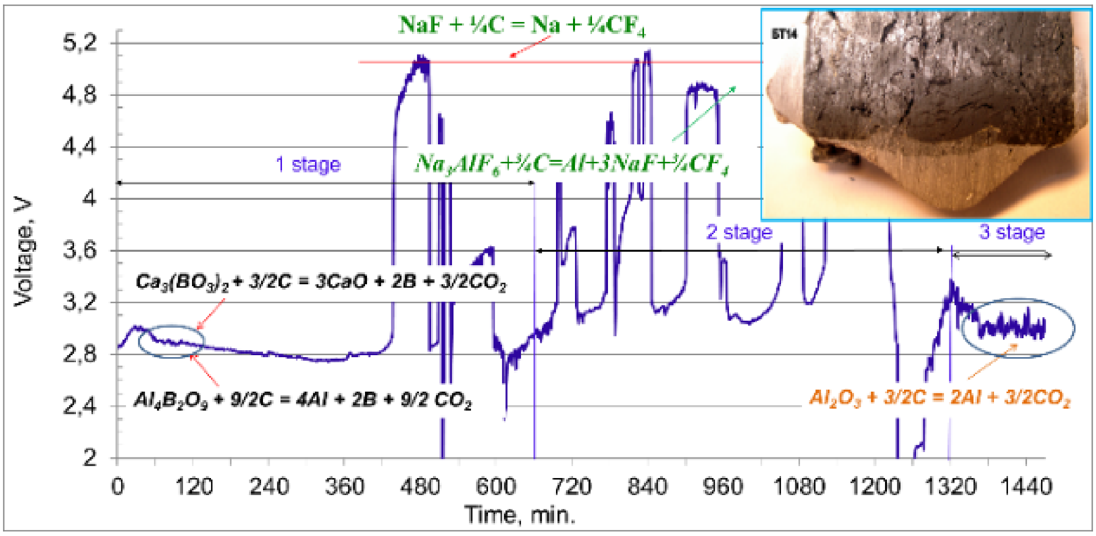

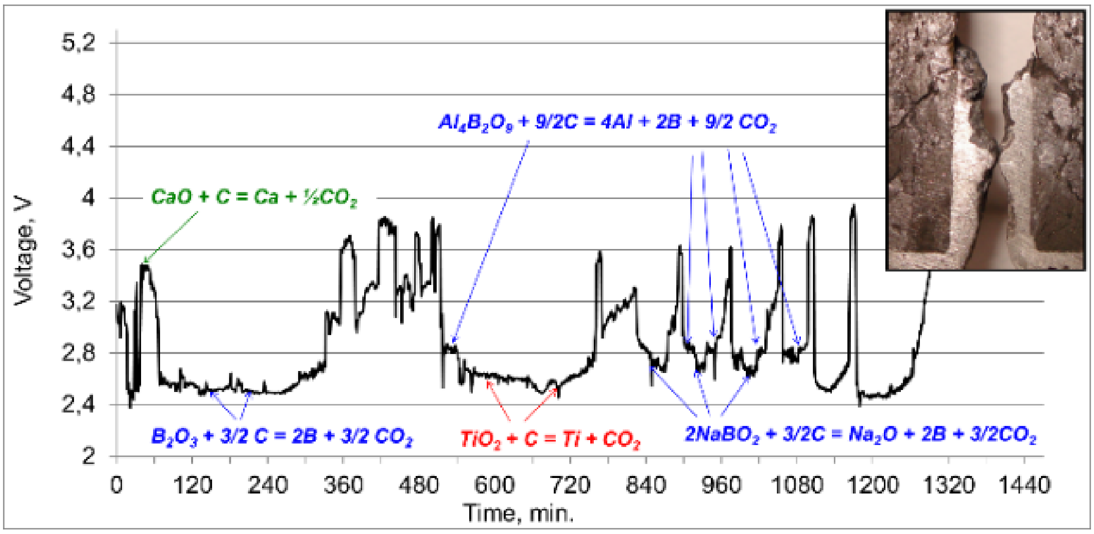

Figure 21. Dynamics of experimental voltage. Top: Cathode milled without polishing, Bottom: Cathode with a polished surface. Note that decimal comma is used on vertical axis instead of decimal point.

A sharp and regular increase in voltage to 3.5 – 5 volts indicates a shift in the cathode potential to the values of the decomposition potentials of the most electronegative impurity components, such as calcium, and electrolyte components.

This spontaneous voltage increase to the discharge of the most electronegative components is usually explained by the concentration polarization of the cathode; although, in this case, the content of constituents of electroactive components in the electrolyte volume did not significantly change during the whole experiment (XRD of electrolyte samples).

However, there is another mechanism for the occurrence of cathodic concentration polarization associated with the quality of the electrode surface. In the examination of carbon cathodes after experiments using electron microscopy, a high surface microdefect occurrence was detected in all cases (Figure).

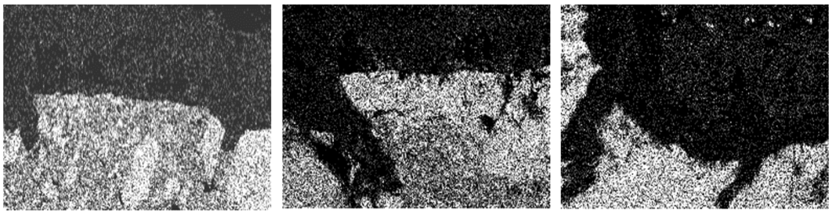

Figure 2. EDS-mapping of the cathode carbon surface after electrolysis (×55 enlargement).

The developing initial physical inhomogeneity of the surface generates a high fluctuating current density on micro-sites of micro-defects. With the development of the process, this is transformed into a real cathode current density, sharply increasing the speed of the target processes at the cathode (1), (2) and the reduction of aluminum. This, in turn, creates an inevitable deficit of electroactive ions in the cathode diffusion layer with the subsequent development of the discharge processes of the most electronegative components of the melt, and in the limiting case, the decomposition of cryolite, sodium fluoride and aluminum.

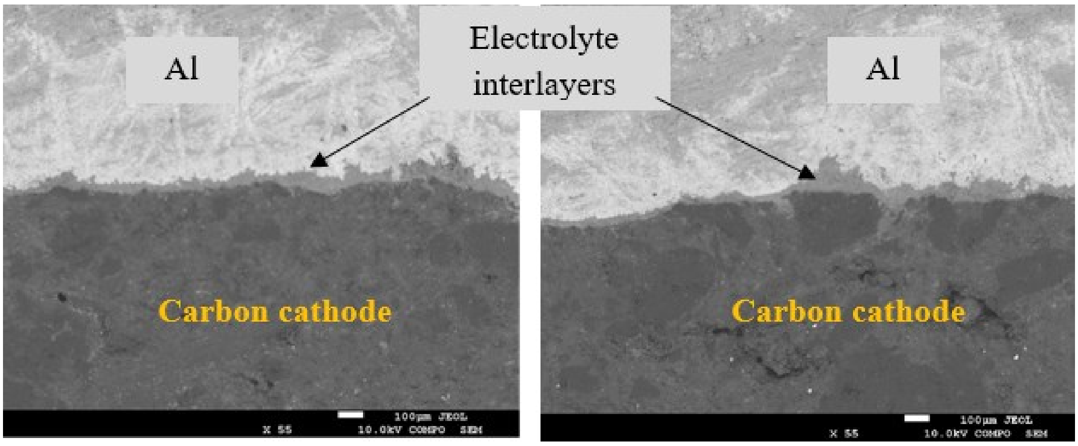

Figure 3. SEM cathode sections after experiments (× 55 enlargement).

After removing the sample from the cell, a layer of aluminum with satisfactory adhesion to carbon was detected on the submerged part of the cathode. This result could be considered successful and acceptable for the implementation of technology on an industrial scale. However, on closer examination (SEM-EDS analysis), the observed wettability can be qualified as “pseudo-wettability” since the contact of aluminum with the surface is realized through an electrolyte layer of discrete thickness of 50 – 500 μm (Figure 3).

3.1. Wettability, Pseudo-Wettability and Cathode Passivation

The dynamics of cell voltage and the results of electron microscopy studies of the surface of carbon cathodes reveal the relationship between the unstable mode of electrolysis processes using solid cathodes, the state of their surface, and the aluminum – cathode interface (Figures 1 - 3). Obviously, the main reason for the inconclusive results of many years of research by various authors [10 - 13] as well as those of our attempt to create aluminum-wettable coatings by electroplating is the extremely non-uniform surface of carbon materials with numerous micro and macro irregularities, cracks and pores (Figure).

This surface is covered with large-size extruded or cast cathode products made from aluminum-wettable materials that have been tested for a long time and are intended to be used in a new generation of cells with drained cathodes and with vertical arrangement of electrodes. Also, this circumstance requires a detailed consideration of the probable mechanisms for the formation of the interfacial electrolyte layer ("pseudo-wettability") by two separately or jointly operating mechanisms - capillary and electrochemical.

3.2. Capillary Mechanism of "Pseudo-wettability" Formation

In an aluminum cell, the so-called immersion wetting of the electrode surface with electrolyte and aluminum melts takes place. Here, two phases are involved: a liquid and a solid. Wettability manifests itself by partial or complete spreading of aluminum and electrolyte over the cathode solid surfaces and by impregnation into their porous structure; and it is characterized by a wetting angle between melts and cathodes ($\theta_{Al\text{-}Cat}$, $\theta_{bath\text{-}Cat}$), a surface tension of aluminum (σ_{Al}, *N/m*) or electrolyte (σ_{bath}, *N/m*) and the adhesion of melts to the solid surface of the electrodes.

The specific work of adhesion (W_{ad}, *N/m*) is defined as the energy required to separate solid and liquid surfaces, i.e., a measure of the adhesion strength of a solid and a liquid body. All these parameters are related by the Equation (4):

$$W_{ad} = \sigma \cdot (1 + \cos\theta_{Al(bath)-Cat}) \qquad [N/m] \qquad (4)$$

As a result of the adhesive interaction, the system becomes two-phase, and the initial Gibbs energy decreases by an amount equal to the molar work of adhesion:

$$\Delta G + W_{ad}(mol) = 0 \qquad \Delta G = -\,W_{ad}(mol), \qquad [J/mol] \qquad (5)$$

To a large extent, the results of wetting depend on the ratio of the adhesion work to the opposite work of cohesion (W_{koh}, N/m), performed by the forces of mutual linkage of the molecules of the liquid. To overcome them, it is necessary to expend twice the energy of the surface tension of aluminum or electrolyte:

$$W_{koh} = 2 \cdot \sigma_{Al(bath)} \qquad [N/m] \qquad (6)$$

The difference between the work of adhesion and cohesion is called the work of spreading:

$$W_{spr} = W_{ad} - W_{koh} \qquad [N/m] \qquad (7)$$

The interaction of porous polycrystalline products with molten salts is accompanied by the impregnation of the porous structure. This process is determined by the capillary pressure P_c of electrolytes [14]:

$$P_c = \frac{2 \cdot \sigma_{bath} \cdot cos\, \theta_{bath}}{r} \qquad [Pa] \qquad (8)$$

where r is the capillary radius (pores), m.

Thus, the existing theory for the interaction of liquid phase with the solid surface and the known values of the surface tension of the melts help estimate in some systems the wetting angles θ and represent the behavior of the system at the interface. However, in most cases, in the absence of chemical interaction, the wetting angles are determined by experimental methods. Then, in the reverse order, for the known θ and σ, the adhesion and cohesion works are calculated.

Table 1. Wetting characteristics of solid surfaces with aluminum and cryolite.

System	Temperature, °C	Environment	Θ, degree	Reference
Al – C	900 - 1000	Ar, vacuum	> 90	[15]
	1200	Ar, vacuum	38	
Al – TiC (dense)	900 - 1000	Vacuum	60 - 100	[16, 17]
	> 1000		→ 0	
Al – TiB_2 (dense)	940 - 1000	Vacuum	20 - 37	[18, 19]
Al – ($60TiB_2$+40C)	1000	Electrolyte	53	[20]
Cryolite – TiB_2	1050	Ar	39	[21]
Cryolite – TiC	1050	Vacuum	19	

Literature data on the surface tension of aluminum also show a significant spread in the range of 850 - 1100 mN/m [22]. The temperature dependence of surface tension presented in [23-25] was used in the calculations of adhesion and cohesion characteristics of aluminum and electrolyte.

After a short start-up and initial period of operation of the electrolysis cell, the heat balance is established, the rate of impregnation and saturation of the cathode with electrolyte components stabilizes, and a layer of aluminum of various thicknesses is formed on the cathode surface:

- From 10 to 40 cm with a horizontal arrangement of electrodes (aluminum "pad");
- Up to 1 cm on the sloped surface of the drained cathode structure; and
- A thin layer of 1-4 mm on the vertical cathodes.

The aluminum layer blocks free access of the cryolite – alumina melt to the electrode surface. A new dynamic equilibrium of transfer for the main components of the melt (Na, Na_3AlF_6, NaF, AlF_3) and dissolved impurities is established in the polycrystalline structure of the material, at which the filtration rate and the melt movement in the cathode body slow down and then stabilize. It is the redistribution of the filtrate that causes reactive forces in the surface layers of the cathode in the closed pore and in the defective structure of the mono-layer material or composite. These forces are equal to the capillary pressure and directed towards the aluminum layer on the horizontal or vertical surface. In the same direction, cohesion forces work on the interfacial surface of aluminum. Under these conditions, part of this filtrate can be extruded onto the interfacial surface of the aluminum-cathode into a thin and evenly or discretely-distributed electrolyte layer. In the opposite direction, the adhesion force and the hydrostatic pressure of the molten aluminum and electrolyte occur in the conventional design of the electrolysis cell, or those of the electrolyte in the vertical arrangement of the electrodes.

Thus, in the cell at the interface of the liquid aluminum – cathode, opposite pairs of forces act:

- Adhesive and cohesive forces;
- Capillary and hydrostatic pressure.

Under the condition of dynamic equilibrium of acting forces on an area equal to the average area of one pore S_{por}, the following equation can be written:

$$(P_c - P_{hydr}) \times S_{por} = (W_{ad} - W_{koh}) \times h_0 \qquad [N] \qquad (9)$$

where $P_{hydr} = \rho g H$: total hydrostatic pressure, Pa; $H = h_{bath} + h_{Al} + h_0$: h_{bath} and h_{Al} , height of electrolyte and aluminum layers, respectively, *m*; h_0: height (thickness) of the electrolyte layer at the aluminum-cathode interface, *m*; ρ: density of Al and electrolyte melts, kg/m^3; g = 9.8 m/s^2: gravitational acceleration; $S_{por} = \pi \cdot r^2$: average dead-end pore area, m^2.

The left part of Equation (9) represents the force acting on the limited surface of the aluminum or the cathode, equal to S_{por}. The direction of the vector of this force, in the direction of aluminum or cathode, depends on the ratio of capillary and hydrostatic pressures, that is, the characteristics of the wetting of the surface of the cathode electrolyte and the heights of the aluminum melt layer and the electrolyte.

The right side of Equation (9) is the force that moves the aluminum surface over a distance of h_0. The direction of this force depends on the ratio of the adhesion and the cohesion forces of the aluminum surface adjacent to the cathode surface. Substituting Equation (7) and P_{hydr} into Equation (9), a formula for calculating the thickness of the electrolyte layer at the aluminum-cathode interface is obtained:

$$h_0 = \frac{S_{por} \times (\mathrm{P}_c - \mathrm{P}_{hydr}^{Al-bath})}{W_{spr} + \rho \cdot g \cdot S_{por}} \cdot 10^{-6} \qquad [\mu m] \qquad (10)$$

where $\mathrm{P}_{hydr}^{Al-bath} = \rho g(h_{bath} + h_{Al})$: hydrostatic pressure of the electrolyte and aluminum melt layer.

In Equation (10), the term in the numerator $\rho g S_{por}$ has values in the order of ~ 10^{-4} and practically does not affect the final results (in 3rd or 4th decimal places). Therefore, the final equation for calculating the thickness of the electrolyte layer can be taken as:

$$h_0 = \frac{S_{por} \times (\mathrm{P}_c - \mathrm{P}_{hydr}^{Al-bath})}{W_{spr}} \cdot 10^{-6} \qquad [\mu m] \qquad (11)$$

Calculation of h_0 was performed for carbon graphite cathodes and cathodes of titanium carbide *TiC* and diboride TiB_2 with horizontal and vertical electrodes. It was assumed that the following reactions occur at the interface between aluminum and cathodes:

$$4Al + 3C = Al_4C_3 \qquad \Delta G^0_{1200} = -140\ kJ/mol \qquad (12)$$

$$13/3Al + TiC \rightarrow Al_3Ti + 1/3Al_4C_3 \qquad \Delta G^0_{1200} = +3\ kJ/mol \qquad (13)$$

$$4Al + TiB_2 \rightarrow Al_3Ti + AlB_2 \qquad \Delta G^0_{1200} = +143\ kJ/mol \qquad (14)$$

Thermodynamic conditions for the interaction of aluminum with a carbon cathode ($\Delta G^0_R < 0$) allow them to be used as initial data for calculating the wetting characteristics and the parameter h_0 depending on temperature, levels of aluminum and electrolyte melts, and pore sizes of polycrystalline cathodes. For the calculation of the probable formation of h_0 during the interaction of aluminum with the *TiC* and TiB_2 cathode, the starting point was the literature data on the wetting of titanium carbide-diboride with aluminum (Table).

According to the results of the calculation, the dynamics of the electrolyte layer formation at the aluminum – cathode (*Al-C*) interface is directly proportional to the local temperature (Figure). Moreover, the space between *Al – C* decreases with a decrease in temperature, which is explained by the increasing adhesion of aluminum to carbon due to the development of interaction (reaction given by Equation (*12*) with a decrease in temperature within the working range.

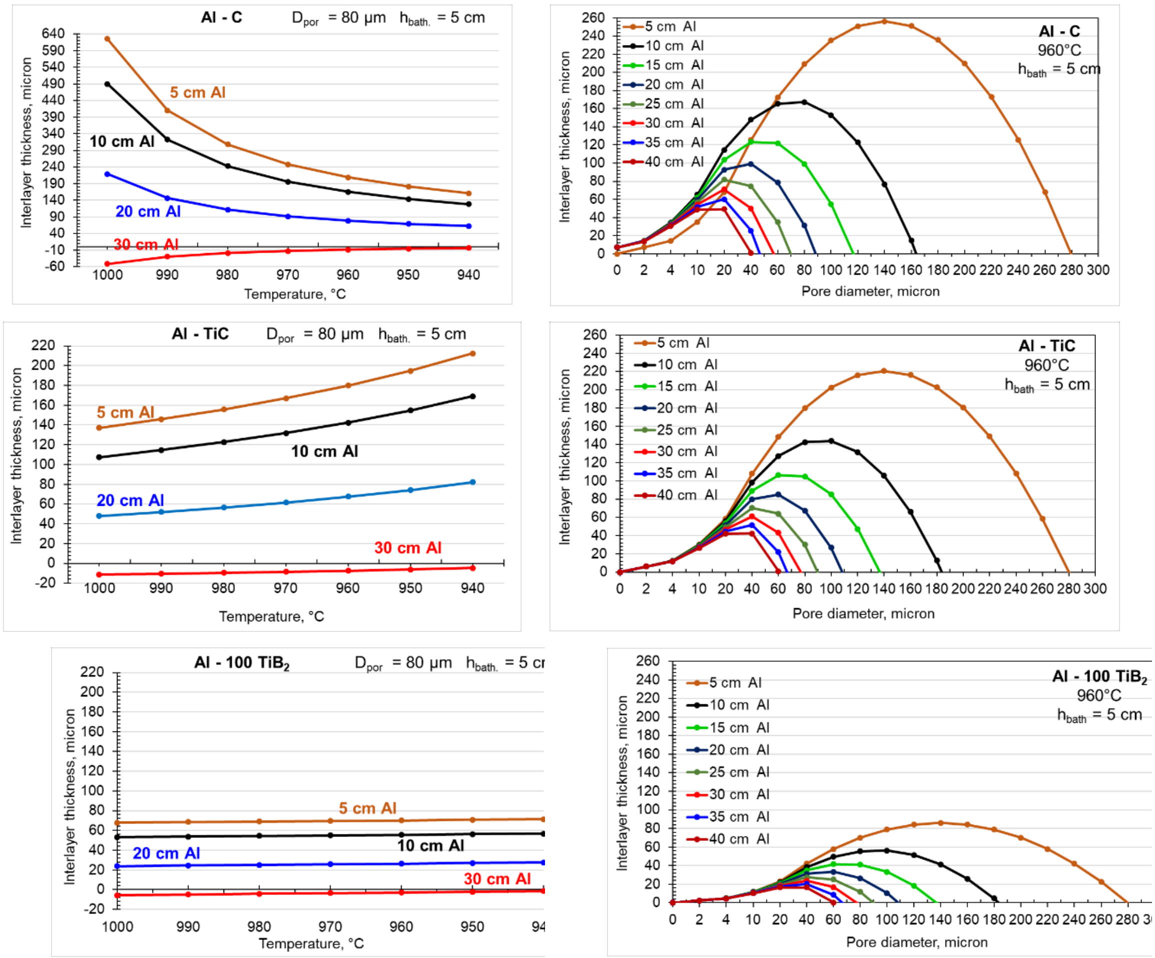

$h_0 = f(T, h_{Al})$

Horiz. Arrang. of Electrodes

$h_0 = f(d_{por}, h_{Al})$

Figure 4. Changing h_0 between the Al and the cathode.

Contrarily, the weak thermodynamic probability of the aluminum interaction with carbide and titanium diboride (reactions given by Equations (13) and (14)) causes the growth of an electrolyte layer between the aluminum layer and the cathode with a decrease in temperature, which is associated with an increase in the surface tension of aluminum as well as in cohesive forces.

At the same time, at the electrolysis process temperature of 960 – 970 °C, the thickness of the interlayer h_0 decreases in the order $C \rightarrow TiC \rightarrow TiB_2$. It should be also noted that, with an increase in the aluminum level at the bottom and an increase in the hydrostatic pressure, the electrolyte layer decreases and does not form when the metal layer is greater than 30 cm. This dependence explains, for example, the more stable operation of Soderberg cells at high aluminum levels of 30–45 cm.

A remarkable relationship is observed between the thickness of the interfacial layer and the pore size. Commonly for composite materials, within the size range of dead-end pores of 40–120 µm, there is a critical diameter at which the interlayer thickness is maximum for each of the aluminum levels at the cathode. It is logical that this maximum decreases with increasing hydrostatic pressure (aluminum level) and with the transition from the carbon cathode to TiC and TiB_2. At large and small capillary diameters, h_0 tends to zero as the pore size increases and the capillary pressure decreases; as the pore sizes or defects approach from 40 to 2 µm, the thickness of the interlayer decreases due to the physical resistance of the liquid phase transfer.

A similar effect of temperature, size of the pore structure and height of the electrolyte melt on the thickness of the layer is also observed for vertical electrodes since the location of the impregnation of the electrodes, the characteristics of materials, electrolyte and aluminum do not change due to the location of the cathodes. The difference lies in the thickness of the aluminum layer on the cathode surface. For a vertical electrode, it was assumed that the wetting of the surface at varying degrees provides a thickness for the flowing aluminum layer ranging in height from 1 to 4 mm. Capillary pressure, more precisely its reverse reaction, is counteracted by aluminum adhesion and hydrostatic electrolyte pressure of various heights.

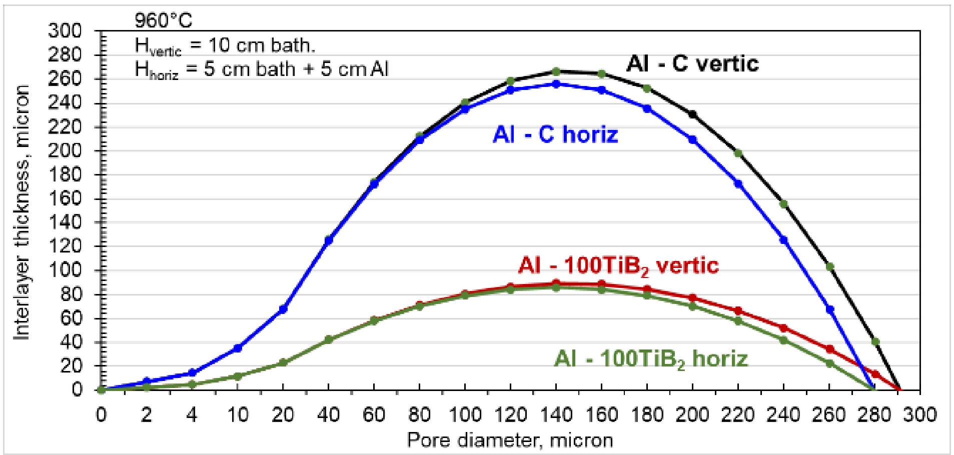

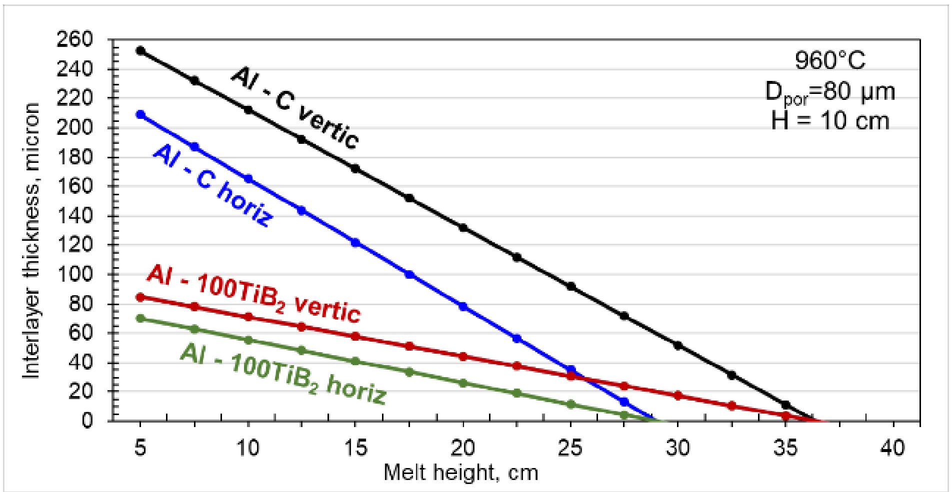

Figure 5. Comparative h_0 dynamics on horizontal and vertical cathodes.

Therefore, the absolute values of h_0 for vertical cathodes in all cases are slightly higher than those with the combined formation of P_{hydr} due to aluminum and electrolyte layers. And this can be clearly seen in the graphs (Figure). In addition, the thickness of the interfacial layer will vary along the height of the cathode from the maximum values near the electrolyte surface to the minimum and total absence in the lower part of the cathode, for the case here, after 35 cm of immersion depth.

Thus, on polycrystalline cathodes with the existing structure of dead-end pores and intergranular defects, an electrolyte layer is formed on the aluminum-cathode interface between 20 and 500 µm thick, regardless of the material. As a result, the observed effect of "pseudo-wetting" and the passivation of the cathode surface take place.

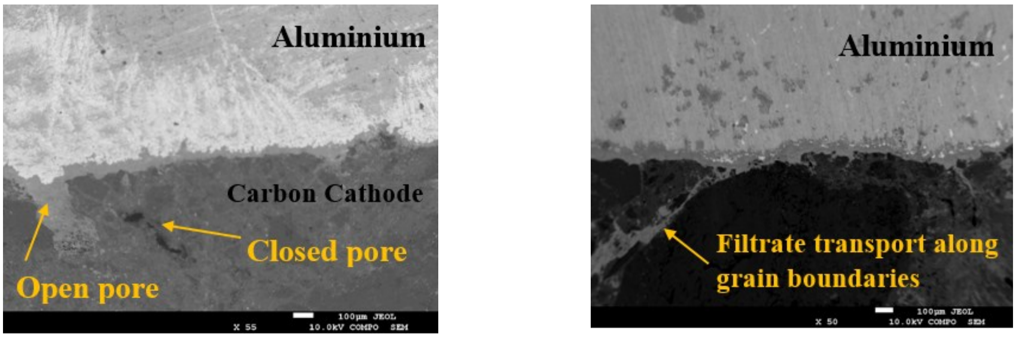

Figure 22. The microstructure of the carbon cathode after the experiment, (x 55 magnified).

On carbon cathodes, one can clearly observe the electrolyte layer between aluminum and the cathode surface, which is fed by the melt filtrate from the surface of the dead-end pores and the sample volume along the grain boundaries (Figure 22). The products of the interaction of aluminum with its surface dissolve in this layer, which, during prolonged operation, can cause the cathode to be passivated and disrupt the normal electrolysis process.

Considering that, for cathodes of TiC and $100\ \%\ TiB_2$, wetting characteristics for dense hot-pressed products were used in the calculations (Table), the problem of “pseudo-wetting” also exists for less porous polycrystalline cathodes. The formation of an electrolyte layer cannot be ruled out on a non-porous, for example, cast surface of a cathode by an electrochemical mechanism. This mechanism is implemented on a chemically inhomogeneous surface, which in an aggressive environment over time is transformed into a physical microdefect.

3.3. Electrochemical Mechanism of the "Pseudo-wettability" Formation

Chemical macro and microdefect products are formed in the presence of the filler, oxide films and inclusions of varying intensity on the surface and at the grain boundaries. The main operational problem for the development of technology of cells with vertical electrodes is not an inert anode, but a hot-pressed TiB_2 cathode [26]. The essence of the problem is not revealed, but the presence of oxides in dense cathode products that appear during their manufacture as well as during the firing and start-up of the cell is indicated and investigated.

In [27, 28], the authors recorded large differences in the resistance of TiB_2 ceramics to the corrosive effects of aluminum, depending on the secondary phases present in the structure. At 1000 °C, they observed the penetration of aluminum into compact TiB_2 containing the secondary phase of the oxycarbide $TiC_{1-x}O_x$ and titanium carbonitride Ti_2CN along the grain boundaries. When this happens, the degradation of all the initial properties of dense titanium diboride occurs. In this context, it should be noted that aluminum reduction processes on indifferent solid cathodes (for example, tungsten or titanium diboride) occur in two stages [25]:

Stage 1 $Al^{3+} + 2e \rightarrow Al^{+}$ (15)
Stage 2 $Al^{+} + 1e \rightarrow Al$ (16)

The presence within the cathode space of extremely aggressive aluminum ions Al^{+} repeatedly increases the destructive effect of aluminum according to the mechanisms investigated by the authors [27, 28]. In addition, in this case, not only the cathodes will be exposed to the corrosive effect, but also the anodes as well located at a minimum distance.

In the presence of physical microdefects, the direct current is concentrated on narrow faces, edges, microcracks, pores or point areas of protruding micro-inhomogeneities. Over the entire surface, a high fluctuating current density arises; and with the possibility of development of physical micro-defects, this is transformed into a reality, even exceeding not only the geometrically calculated value, but also that for the maximum diffusion for the discharge of aluminum. These processes were repeatedly observed when the results of experiments were analyzed.

Visually, on the graphs of continuous voltage fixation in the system, they are expressed by gradual or abrupt voltage increases of up to 4 - 5 volts, simultaneously or continuously for 30 – 120 minutes (Figure 1). At such high real current densities, under conditions of concentration polarization, powder precipitates of titanium diboride or the most electronegative impurity electroactive components will form on the cathode, for example:

$CaO + C = Ca + \frac{1}{2}CO_2$ $E^0_{1200} = -1.657\ V$ (17)
$CaO = Ca + \frac{1}{2}O_2$ $E^0_{1200} = -2.639\ V$ (18)

In turn, these elements with high probability can interact with the cathode material or its components:

$Ca + 2C = CaC_2$ $\Delta G^0_{1300} = -6.25\ kJ/mol$ (19)

$Ca + 6B = CaB_6 \qquad \Delta G^0_{1300} = -533.81\ kJ/mol,$ (20)

forming an insulating layer.

In addition, under conditions of concentration polarization and enrichment of the cathode electrolyte volume with sodium ions, they are discharged on an inert cathode with subsequent interaction with the surface material:

$TiBO_3 + Na = NaBO_2 + TiO \qquad \Delta G^0_{1200} = -33.50\ kJ/mol$ (21)
$3TiB_2 + Na = NaB_6 + 3Ti$ (22)

These probable processes also change the composition of the cathode surface, passivating it with sodium metaborate $NaBO_2$ ($T_{melt.}$ = 966 °C) and/or sodium hexaborate NaB_6, which is an insulator with a specific electrical resistance of about $4×10^4$ Ωm [29]. A partial or complete dissolution of sodium borate $NaBO_2$ in the electrolyte will increase the microdefect of the cathode. This process was confirmed by the results of special studies of the authors [30].

Summarizing, the macro- and micro-sites of the cathode surface of mono-materials or composites have an initial physical microdefect as well as greater or less reactive activity with respect to the aggressive components of the working environment. During long-term operation in an aggressive environment, that is, with the development of chemical microdefects and progressive surface and volume heterogeneity, decomposition of electrolyte components on reactive cathodes is possible at the cathode:

$AlF_3+¾C=Al+¾CF_4 \qquad E^0_{1200} = -2.193\ V$ (23)
$Na_3AlF_6+¾C=Al+3NaF+¾CF_4 \qquad E^0_{1200} = -2.564\ V$ (24)
$NaF + 1/4C = Na +1/4CF_4 \qquad E^0_{1200} = -2.754\ V$ (25)

or on inert cathodes :

$AlF_3 =Al+¾F_2 \qquad E^0_{1200} = -4.112\ V$ (26)
$Na_3AlF_6 =Al+3NaF+¾F_2 \qquad E^0_{1200} = -4.510\ V$ (27)
$NaF = Na +1/2F_2 \qquad E^0_{1200} = -4.673\ V$ (28)

with corresponding negative consequences for cathodic processes and the state of the electrodes. These effects, under conditions of passivation of the electrode with impurity deposits and enrichment of the volume of the melt and in the near-electrode region with sodium fluoride, will be expressed in terms of the interaction of the impurity elements with the cathode material and as a local increase in the melting point of the melt in the cathode space. As a result, the surface will not only change its composition and physical state, but will also be passivated by electrolyte freezing on the electrode and refractory impurity compounds. These phenomena were observed in our experiments and were recorded by the authors [31] in an experimental simulation of electrolysis in a cell with vertical electrodes of titanium diboride. Ultimately, the normal electrolysis process is disturbed, followed by a need to stop.

Thus, solid polycrystalline cathodes from individual compounds or their compositions cannot be *unconditionally* used for the electrolysis of cryolite-alumina melts in any design, whether horizontal or vertical.

The logical *condition* for their use is the organization of the processes of continuous restoration of the cathode surface, mitigation of its chemical heterogeneity and micro-defects during the entire period of electrolysis. For example, for cathodes based on titanium diboride, the electrolysis technology of cryolite-alumina melts should be accompanied by micro-dosing of boron into the electrolyte, its restoration at the cathode with subsequent interaction on the surface and in the volume of the electrode with impurity components:

$2B + Ti = TiB_2 \qquad \Delta G^0_{1300} = -320\ kJ/mol \qquad (29)$

$3B + TiBO_3 = TiB_2 + B_2O_3 \qquad \Delta G^0_{1300} = -228\ kJ/mol \qquad (30)$

$4B + TiO_2 = TiB_2 + B_2O_2\uparrow \qquad \Delta G^0_{1300} = -119\ kJ/mol \qquad (31)$

$2B + TiC_{0,5}O_{0,5} \rightarrow TiB_2 + 1/2CO \qquad \Delta G^0_{1300} = -81\ kJ/mol \qquad (32)$

These processes will not only restore the original composition of the cathode, but also eliminate the microdefects of its surface.

Under laboratory conditions, this technology was successfully implemented in the method of continuous boronization of carbon titanium-containing cathodes [32, 33]. The mechanism of formation of the cathode layer wetted by aluminum $Ti – B – C$ and its continuous restoration is realized through the series-parallel stages of the opposing solid-liquid and liquid-phase flows of boron and titanium (in elementary form and as compounds), followed by the interaction between them (given by Equations (29) – (32)) and with a composite base:

$2B + TiO_2 + 2C \rightarrow TiB_2 + 2CO \qquad \Delta G_{1300K} = -67.0\ kJ/mol \qquad (33)$

$B_2O_3 + Ti + 3C \rightarrow TiB_2 + 3CO \qquad \Delta G_{1300K} = -41.0\ kJ/mol \qquad (34)$

In the near-surface volume of the carbon cathode, it is intended to create a continuous, durable, constantly reproducible titanium diboride layer. The generation of a wettable layer does not depend on the quality of the surface on which it is created. Microboring of the cathode and organization of electrochemical reactions on the surface restore its quality, reducing its chemical heterogeneity and micro-defectiveness during the entire period of electrolysis. Therefore, the technology of boring titanium-containing cathodes eliminates the appearance of the effect of "pseudo-wetting", that is, the formation of liquid aluminum–solid cathode of the electrolyte layer at the interface.

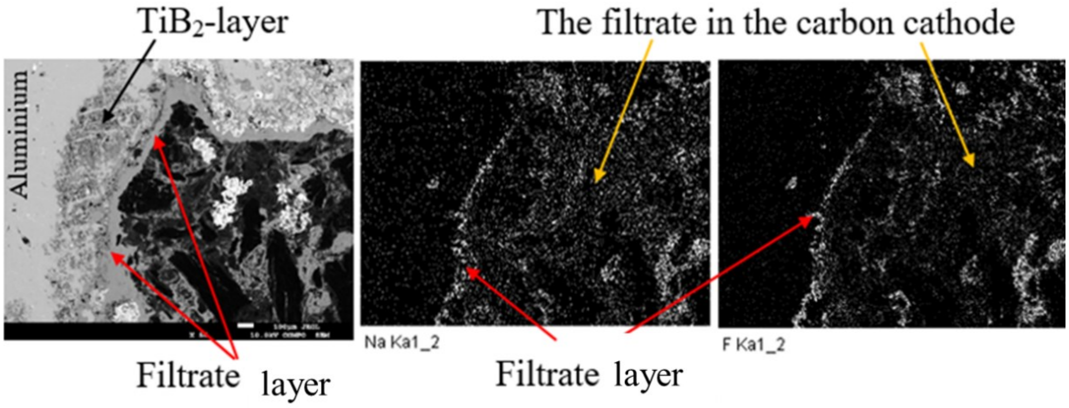

Figure 7. Aluminum wetted TiB_2-layer and distribution of filtrate in the cathode body.

The redistribution of the filtrate occurs in the cathode volume. A dense TiB_2 layer with pores of 2-µm diameter, as stated in [32, 33], does not allow the electrolyte filtrate to penetrate into the Al

– C interface. This process is fixed on the photo of the microstructure and EDS-maps of sodium and fluorine (Figure). The filtrate is distributed along the grain boundaries of the filler and a layer of about 50 microns is concentrated under the TiB_2 layer.

Carbon-titanium and boron-containing cathodes and anodes can be manufactured at the electrode and the anode plants with a dosage in the composition of titanium and boron-containing compounds. Both titanium diboride and composite compositions TiB_2 - *CG* (Titanium Diboride–Carbon Graphite) obtained using low-temperature synthesis of titanium diboride can be used as cathodes [34, 35].

4. Conclusions

1. The technology of electrochemical deposition of boron, titanium and aluminum on a carbon cathode from cryolite-alumina melts at ~970°C and a current density of 0.82 A/cm^2 provides a visual effect that resembles wetting of the electrode with aluminum. The results of the process are directly dependent on the surface quality of the polycrystalline cathode.
2. The long-term lack of progress in the commercial development of the technology for the electrolysis of cryolite-alumina melts using inert electrodes has been explained by specific electrochemical processes on the cathode surface.
3. Chemical and physical inhomogeneity of the cathode surface is the cause of the periodic occurrence of concentration polarization and the instability of electrochemical processes, the consequences of which are closely linked to the interaction of impurity elements with the cathode material and the decomposition of electrolyte components. As a result, the cathode surface not only changes its composition and physical state, but is also passivated by refractory impurity compounds and electrolyte freezing on the electrode.
4. The established causal relationship between the heterogeneity of the electrode surface and the instability of the cathode process gives grounds to state:
    - Solid polycrystalline cathodes from individual compounds or their compositions cannot be *unconditionally* used for the electrolysis of cryolite-alumina melts in any design, whether horizontal or vertical.
    - The logical *condition* for the use of solid cathodes is the organization of electrolysis processes with continuous surface restoration, which reduces its chemical heterogeneity and micro-imperfection during the entire operational period.
5. For technological and constructive development of new generation cells, it is proposed to use the technology of continuous micro-boronization of the surface of individual TiB_2 or composite $TiB_2 - CG$ cathodes manufactured using the technology of low-temperature synthesis of titanium diboride.

5. References

1. A.I. Belyayev and Ya. V. Studetsov, Electrolysis of alumina with non-consumable (metallic) anodes, *Light Metals* 1936, No.3, 15-24. (Беляев, А.И. Электролиз глинозема с несгораемыми (металлическими) анодами / А. И. Беляев, Я.В. Студенцов // Легкие металлы. – 1936. – № 3. – С. 15-24).
2. A.I. Belyayev and Ya. V. Studentsov, Electrolysis of alumina with non-consumable oxide anodes, *Light Metals* 1937, No.3, 17-21. (Беляев, А.И. Электролиз глинозема с несгораемыми анодами из окислов / А. И. Беляев, Я.В. Студенцов // Легкие металлы. – 1937. – № 3. – С. 17-21).
3. A.I. Belyayev, Electrolysis of alumina with non-consumable ferrite anodes, *Light Metals* 1938, No.1, 7-20. (Беляев, А.И. Электролиз глинозема с несгораемыми анодами из ферритов / А. И. Беляев // Легкие металлы. – 1938. – № 1. – С. 7-20).

4. Pat. Spec. 802905 GB. Int. Cl. B23n. C22d. Improvements in or relating to Electrolytic Cells for the Production of Aluminium / Ransley C.E. – Appl. No. 1155/54; Jan. 14, 1954; Filed: Jan. 14, 1955; Date of Patent: Oct. 15, 1958. – 8 p.
5. C.E Ransley, The Application of the Refractory Carbides and Borides to Aluminum Reduction Cells, *Extractive Met. of Aluminum*, Vol. 2, Aluminium, New York: Interscience, 1962. – P. 487-506.
6. An Aluminum Revolution / T.M. Leeuwen // *Equity Research Report, Credit Suisse First Boston Corporation.* – June 22, 2000. – 110 p.
7. Aluminium producers promise a cleaner smelting pot / *Nature* 557, 280 (2018) / https://www.nature.com/articles/d41586-018-05158-1.
8. D.A. Simakov et al., Creation of electrolysis technology with inert anodes, *II International Congress "Light Metals* 2010", 2 – 4 September 2010, Krasnoyarsk, 546-554. (Симаков, Д. А. Создание технологии электролиза на инертных анодах / Д. А. Симаков, А. В. Фролов, А. О. Гусев // II Международный конгресс «Цветные металлы-2010», 2-4 сент., г. Красноярск. – 2010. – С. 546-554).
9. E.S Gorlanov et al., Development of technology for Al-wettable coating on a carbon cathode, *Proceedings of 31st International ICSOBA Conference*, Krasnoyarsk, Russia, 4 – 6 September 2013, 634-658. (Горланов, Е. С. Разработка технологии создания Al-смачиваемого покрытия на углеродном катоде. Часть 1-2. / Е.С. Горланов, Г. В. Архипов, А. М. Иванова // Сб. научн. статей XXXI Междун. конф. «ИКСОБА» и XIX Междун. конф. «Алюминий Сибири» /Под ред. П. В. Полякова и А. В. Панова – Красноярск: Версо, 4-6 сентября 2013 г. – стр. 634-658).
10. S.C. Raj and M. Skyllas-Kazakos, Electrochemical studies of the effect of TiO_2 and B_2O_3 additions on the aluminium deposition reaction in the molten cryolite bath, *Electrochimica Acta*, 1992, Vol.37, 1787-1796.
11. M. Makyta et al., Electrodeposition of titanium diboride from fused salts, *Journal of Applied Electrochemistry* 1996, Vol. 26, 319-324.
12. S.V. Devyatkin et al., Electrochemical synthesis of titanium diboride coatings from cryolite melts, *Molten Salts Forum; Trans Tech Publications*, 1998, Vols. 5-6, 331-334.
13. G. Kaptay and S.V Devyatkin, On possibility of preparation of titanium diboride cathode coating in situ in the aluminium electrolysis cell by electrochemical synthesis, *Proceedings of 8 Int. Congress of ICSOBA,* 1997, Vol. 24, 135-144.
14. A.P. Belyayev et al., *Physical chemistry of molten salts*, Metallugizdat, 1957, 359 pages. (Беляев, А. П. Физическая химия расплавленых солей / А. П. Беляев, К. А. Жемчужина, Л. А. Фирсанова. – М.: Металлургиздат, 1957. – 359 с.)
15. V.A. Doktyushin et al., Contact interactions in composite materials, Tutorial, BolgGTU, BVolgograd 2003, 74 pages. (Локтюшин, В.А. Контактные взаимодействия в композиционных материалах: Учебное пособие / В.А. Локтюшин, Н. А. Адаменко, Л. М. Гуревич // ВолгГТУ, Волгоград, 2003. – 74 с).
16. V.G. Babkin, A Terentsev, A.I. Prefileva, Casting of metal-matrix composite materials for electrical applications, (Бабкин, В. Г. Литые металломатричные композиционные материалы электротехнического назначения / В. Г. Бабкин, Н. А. Терентьев, А. И. Перфильева //) *Journal of Siberian Federal University. Engineering & Technologies*, 2014, Т. 4, № 7, 416-423.
17. N.S. Zyukin, G.A. Kolisnichenko, Adhesion of Mets and brazing of materials, 1986, Issue 16, 22-25. (Зюкин, Н. С. Колисниченко Г. А. / Н.С. Зюкин, Г. А. Колисниченко // Адгезия респлавов и пайка материалов. – 1986. – Вып. 16. – С. 22-25).
18. S.K. Rhee, Wetting of ceramics by liquid aluminum, *J. American Ceram. Soc.*, 1970, Vol. 53, No.7, 386-389.
19. V.I. Mogilenskiy, Research and development of corrosion-resistant materials based on refractory compounds in aluminum melt, The author's abstract Diss. for the degree of candidate of technical Sciences, Leningrad Technical Institute Lensovyeta, Leningrad, 1970, 16 pages. (Могиленский, В. И. Исследование и разработка

коррозионностойких в расплаве алюминия материалов на основе тугоплавких соединений // Автореферат дис. на соискание ученой степени кандидата технических наук. (05.350) / Ленингр. технол. ин-т им. Ленсовета. - Ленинград , 1970. - 16 с.)

20. Xian-an Liao and Ye-Xiang Lin, Same important performances of TiB_2 coated cathode carbon block, *Light Metals* 1990, 409-412.
21. I.E. Veneraki et al., Study of wetting of refractory materials with cryolite, *Ukrainskiy Khimicheskiy Zhurnal*, 1973, Vol. 42, No. 3, 291-292. (Венераки, И. Э. Изучение смачивания тугоплавких материалов криолитом / И. Э. Венераки, А. Д. Панасюк, В. И. Дешко // Украинский химич. журнал. – 1973. – Т. 42. - №3. – С. 291-292).
22. B.B Alchagirov et al., Surface tension of aluminium and its alloys with indium and tin, *Vestnik KBGU*, Series Physical Sciences, Nalchik: KBGU, 2000, Vol 4, 6-10. (Алчагиров Б.Б., Чочаева А.М., Хоконов Х. Б., Таова Т.М., Ибрагимов Х. И. Поверхностное натяжение алюминия и его сплавов с индием и оловом // Вестник КБГУ. Серия Физические науки. Нальчик: КБГУ. -2000. В.4. -С.6-10).
23. O.G. Ashkhotov and A.O Ashkhotov, Surface tension of liquid metals, Rasplavi 2008, No.1, 22-35. (Ашхотов, О. Г. Поверхностное натяжение жидких металлов / О. Г. Ашхотов, А. О. Ашхотов // Расплавы. – 2008. - № 1. – С.22-35).
24. N. Eustathopouos et al, The surface tension of liquid pure aluminium and aluminium–magnesium alloy, *J. Mat. Sci.* 1974, Vol. 9, 1233–1242.
25. M.M Vetyukov, A.M. Tsyplakov, S.N. Shkolnikov, *Metallurgy of Aluminium and Magnesium*, Metallurgiya 1987, 320 pages. (Ветюков М.М., Цыплаков А. М., Школьников С.Н. Металлургия алюминия и магния. - М.: Металлургия, 1987.- 320 с).
26. R. A. Christini et al., Advanced Anodes and Cathodes Utilized in Energy Efficient Aluminum Production Cells, Final Technical Progress Report for Phase III, Cooperative Agreement Number DE-FC07-98ID13666, November 5, 2001, 92 pages.
27. M.S. Jensen et al., Degradation of TiB_2 ceramics in liquid aluminum, *J. Eur. Ceram. Soc.* 2008, Vol. 28, 3155-3164.
28. A. Saai et al., Multi-scale Modelling of Titanium Diboride Degradation Using Crystal Elasticity Model and Density Functional Theory, *Light Metals* 2018, 1329-1336.
29. G.V. Samsonov et al., *Borides*, Atomizdat 1975, 376 pages. (Самсонов Г. В., Бориды / Г. В. Самсонов, Т. И. Серебрякова, В. А. Неронов – М.: Атомиздат, 1975. – 376 с.)
30. Z. Wang et al., Transport of Sodium in TiB_2 Materials Investigated by a Laboratory Test and DFT Calculations, *Light Metals* 2018, 1321-1328.
31. Sh. Bao et al., Effects of Current Density on Current Efficiency in Low Temperature Electrolysis with Vertical Electrode Structure, *Light Metals* 2018, 611-619.
32. E.S. Gorlanov and V.Yu. Bazhin, Nano- and the Microdimensional Coats Polycrystal Titanium-Containing the Bases - A Method of Electrochemical Boronizing, *Smart Nanocomposites*, USA, Nova Science Publishers, Inc. 2016, Vol.7, № 1, 75-88.
33. E.S, Gorlanov, Method of producing and maintaining protective wettable coating on cathode carbon blocks of the electrolytic cell for aluminium production, Russian Patent 2337184, Published 27.10.2008, Bull. Noo. 30, 11 pages. (Пат. 2337184 Российская Федерация, МПК7 C25C 3/08. Способ получения и поддержания защитного смачиваемого покрытия на углеродистых блоках катодного устройства электролизёра для производства алюминия / Е.С. Горланов: Общество с ограниченной ответственностью «Эксперт-Ал». – № 2006142406/02; заявл. 30.11.2006; опубл. 27.10.2008 Бюлл. №30 – 11 с).
34. E.S. Gorlanov et al., Method of obtaining titanium diboride powder, Russian Patent 2603407, Published 30.04.2015, Bull. No 33, 12 pages. (Пат. 2603407 РФ. МПК B22F 9/18, C01B 35/04, C01G 23/00. Способ получения порошка диборида титана / Е.С. Горланов, В.Ю. Бажин, А.В. Смань./ ООО "Эксперт-Ал" - 2015107637/02, опубл. 30.04.2015. – опубл. 27.11.2016, Бюлл. № 33. – 12 с).

35. E.S. Gorlanov, Carbothermal synthesis of titanium diboride, *Zhurnal SFU, Technique and Technology* 2018, No 11, No 2, 156-166. (Горланов, Е. С. Карботермический синтез диборида титана: апгрейд / Е. С. Горланов, В.Ю. Бажин, С. Н. Федоров // Журнал СФУ. Техника и технология. – 2018. - №11. – № 2. – С.156-166).